Research Paper ■

Arm Orthosis Modeling for Exploration of Human-Robot Interaction in Arm Reaching Trajectory Formation

Matjaž Zadravec, Zlatko Matjačić

Abstract. Arm reaching robotic training is usually programmed in a way to assist patients by facilitating movements along a straight line from the chosen starting to the target point. But if we take into account the muscular condition of the patient's upper limb, the trajectories might be different. The key is to find an optimal trajectory. The article presents experimental planar arm reaching movement trajectories obtained by instructing one healthy subject to move the hand from the selected starting to the target point in a relatively narrow workspace. The subject carried an arm orthosis to which we attached elastic bands emulating muscle tightness condition. The results show clear deviations of the trajectories when elastic bands were attached to the orthosis as compared to the uninhibited ones. Clear understanding of human arm motion will aid in better human-machine interaction.

Modeliranje ortoze za raziskovanje interakcije med človekom in robotom pri gibanju roke

Izvleček. Običajni vzorec robotsko podprtega gibanja roke iz točke v točko je ravna trajektorija. Če upoštevamo tudi bolnikovo mišično stanje, pa taka trajektorija ni nujno optimalna. Optimalna trajektorija ima lahko tudi drugačno obliko ali hitrostni profil. V študiji smo pri nevrološko zdravi osebi eksperimentalno zajeli vzorce seganja roke iz točke v točko. V ta namen smo izdelali ortozo za roko, na katero smo pripeli elastične trakove, ki so oteževali delo flektornih mišičnih skupin roke pri gibanju, s čimer smo posnemali okvare mišičja pri boleznih oziroma poškodbah živčevja. Rezultati kažejo na razlike v obliki trajektorij v primerih, ko so bili elastični trakovi nameščeni oziroma odstranjeni z ortoze. Jasnejše razumevanje gibanja roke bo pripomoglo k boljši interakciji med robotom in človekom.

■ **Infor Med Slov**: 2012; 17(2): 1-8

Institucija avtorjev / Authors' institution: Univerzitetni rehabilitacijski inštitut Republike Slovenije – Soča.

Kontaktna oseba / Contact person: Matjaž Zadravec, Univerzitetni rehabilitacijski inštitut Republike Slovenije – Soča, Linhartova 51, SI-1000 Ljubljana. e-pošta / e-mail: matjaz.zadravec@ir-rs.si.

Prejeto / Received: 21.09.2012. Sprejeto / Accepted: 30.10.2012.

Introduction

In the recent years, rehabilitation robots have made their way into clinical practice because they can apply high-intensity, task-specific, interactive treatment with an objective and reliable means of monitoring patient progress. Rehabilitation robots can also evaluate patients' movement performance and assist them in moving the upper extremity through predetermined trajectories in a given motor task.

When doing arm reaching training with the robot device, the robots are usually programmed in a way to assist patients by facilitating movements along a straight line from the chosen starting to the target point. Selection of a straight line between two selected points with bell-shaped velocity profile is based on predictions of the minimum hand jerk model for trajectory formation.[1,2] However, this might only be valid under certain circumstances in practice: short-distant trajectories in narrow workspace with no constraints in movement space (i.e., boundaries of range of motion – ROM), and no constraints in musculo-skeletal system (e.g., spastic arm or any other disorders). On the other hand, there are several studies proposing the approaches incorporating dynamic features (minimum torque change, minimum torque) when trajectories are slightly curved.[3,4]

All of these approaches are usually studied in healthy subjects. However, the trajectories might be different if we take into account the subject's upper extremity muscular condition. The key is to find an optimal trajectory where the patient could perform better during rehabilitation-robotic training. Optimal trajectories with appropriate robotic support should be essential in stroke rehabilitation.

There are also many studies presenting performance-based adaptive algorithms that minimize robotic support during training,[5,6] but these studies focus only on support algorithms (e.g. assist-as-needed algorithms) while trajectories stay predetermined. Furthermore, several motor control studies have been offered as evidence for the hand trajectory formation during arm reaching movements of neurologically unimpaired participants.[7,8]

The aim of our study was to capture and compare planar movements of the upper limb of one healthy subject under two different arm conditions: unimpaired and emulating flexor muscles stiffness. For this purpose, an upper limb orthosis was made, to which we could attach elastic bands. The elastic bands were emulating the arm's stiffness (similarly to tonic spasticity). When recording the unimpaired arm trajectories, the elastic bands were removed from the orthosis.

Methods

Experimental setup

The experimental paradigm was chosen in such a way as to simplify the problem as much as possible in the sense that only two degrees-of-freedom (DOF) were allowed: even wrist movements were prevented by means of an orthosis, and the influence of gravity was kept constant by working in the horizontal plane. Hence, the movements of the arm were reduced to flexion-extension of the elbow and flexion-extension of the shoulder.

One health man, aged 28, participated in the experiment. He was right-handed and free of any known musculoskeletal or neurological abnormalities. Figure 1 shows the experimental setup. The subject was seating in a straight-backed chair in front of the table, which was raised to a shoulder level to allow only planar reaching movements. We used a wide girdle connecting the shoulder and the straight-back of the chair to minimize the displacement of the shoulder joint center. The girdle was not restricting or feeling uncomfortable when moving the arm in the selected working area.

We placed six white rectangle spots on the table in the relatively narrow workspace in front of the

subject, to mark the starting and target points. The subject carried the two-link orthosis on which three elastic bands were attached. The details of the orthosis are presented in the following subsection.

To record the arm movement in space, we used a Vicon MX motion capture camera system, where six cameras were positioned in the laboratory and five wireless markers were used. Two markers were placed on the table, which is shown in top left corner of Figure 1, to determine the coordinate system. The origin of the Cartesian coordinate system was then moved and positioned in the shoulder joint, where the horizontal axis (abscissa) was defined as a vector between these two markers. The vertical axis (ordinate) was then positioned perpendicular to the abscissa. For the arm motion capture, three markers were attached to the arm at the positions of shoulder joint, elbow joint of the orthosis, and the center of the hand (the end of orthosis). The measured data was exported to MATLAB (MathWorks, Inc.) for further analysis.

Figure 1 Experimental setup for recording movement trajectories.

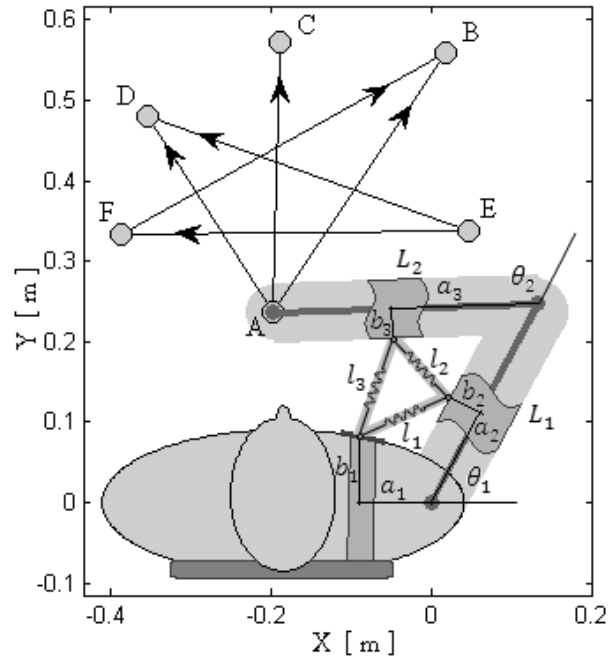

Figure 2 Schematic view of trajectory directions in the arm's workspace and subject with the arm orthosis to which the flector elastic bands are attached.

Orthosis model

To emulate flexor muscle stiffness, the two-link plastic orthosis was made with a single rotation at elbow joint, which is shown in Figure 1 and 2. The orthosis permits moving the arm only in flexion/extension of the elbow joint in the horizontal plane. For this reason, we used three elastic bands – two monoarticular and one biarticular. First elastic band (indexed 1) has its origin at the mounting point fixed on the subject's upper chest, while the other end of elastic band is attached on the orthosis at the link L_1. This elastic band emulates the muscle tightness of monoarticular flexor muscles (especially pectoralis major), and causes the fatigue during arm reaching movements of the shoulder extensor muscles (i.e. posterior deltoid and others). Second elastic band (indexed 2), emulating the brachialis muscle stiffness, connects the arm (link L_1) and forearm (link L_2). It causes the fatigue to the lateral head of triceps brachii. The third elastic band (indexed 3) connects mounting point on the subject's upper chest and the forearm orthosis (link L_2), while its

intention is to emulate biarticular flexor muscle tightness (i.e. biceps brachii) that causes the fatigue of the biarticular extensor muscles (i.e. long head of triceps) during arm reaching movements. The schematic view of the flexor elastic bands attached is shown in Figure 2. All three elastic bands are from the same material with the elastic coefficient of 2.3 N/cm. Figure 3 shows the force-stretch relation of the elastic band, where the 1st order polynomial (linear characteristic) and the 4th order polynomial were fitted on the measured data. For the further calculation of the orthosis characteristics, we used the 4th order polynomial data fit, because it is more accurate than linear fit and it is still simple to differentiate, when we needed to.

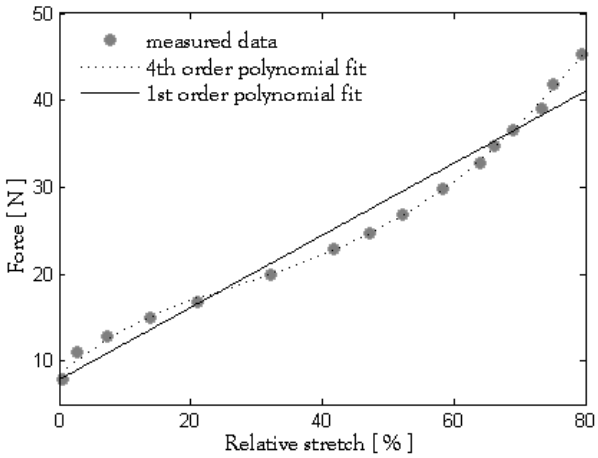

Figure 3 Force-length characteristics of elastic band with polynomial fitting.

Table 1 Segment lengths and orthosis parameters.

Parameter	Value *[m]*
L_1	0.280
L_2	0.330
a_1	0.110
b_1	0.080
a_2	0.152
b_2	0.055
a_3	0.152
b_3	0.040

After the experiment trial, the segment lengths L_1 and L_2 of the arm were measured on the basis of shoulder, elbow and hand markers. The hand marker position of the two-link arm model is expressed by forward kinematics:

$$\begin{bmatrix} x \\ y \end{bmatrix} = \begin{bmatrix} L_1 \cos\theta_1 + L_2 \cos(\theta_1 + \theta_2) \\ L_1 \sin\theta_1 + L_2 \sin(\theta_1 + \theta_2) \end{bmatrix}. \quad (1)$$

The vector of elastic bands' lengths, which depends on the shoulder and elbow joint angles (2) are defined by orthosis parameters a_1, b_1, a_2, b_2, a_3, b_3 and L_1 (Appendix, Table 1).

$$l(\theta) = \begin{bmatrix} l_1(\theta_1) & l_2(\theta_2) & l_3(\theta_1, \theta_2) \end{bmatrix}^T \quad (2)$$

The moment lever matrix can be expressed as follows

$$W(\theta) = \frac{dl}{d\theta}, \quad (3)$$

which represents the Jacobian matrix from the joint space to the elastic bands' space, and has the following form:

$$W^T = \begin{bmatrix} w_1 & 0 & w_{13} \\ 0 & w_2 & w_{23} \end{bmatrix}. \quad (4)$$

The elastic band force vector

$$F(l) = \begin{bmatrix} F_1(l_1) & F_2(l_2) & F_3(l_3) \end{bmatrix}^T \quad (5)$$

is determined from the linear length-dependent characteristics as shown in Figure 3 and (6), where the force begins to work at the nominal elastic band length l_0 onwards with the 4th order polynomial, while it remains zero up to this length.

$$F(l) = \begin{cases} 0 & , \quad l < l_0 \\ p_4 l^4 + p_3 l^3 + p_2 l^2 + p_1 l + p_0 & , \quad l \geq l_0 \end{cases} \quad (6)$$

The polynomial coefficients describing the characteristics of elastic bands and the nominal lengths are given in Table 2. The 4th order polynomials are representative only in the selected narrow workspace of the experiment. Here, the relation between elastic band force vector and

joint torques due to elastic bands stiffness can be represented as follows

$$\tau_{stiff} = W^T F . \quad (7)$$

Table 2 Polynomial coefficients and nominal lengths of elastic bands' characteristics.

	p_4 $[10^5]$	p_3 $[10^5]$	p_2 $[10^5]$	p_1 $[10^4]$	p_0 $[10^2]$	l_0 $[m]$
F_1	-5.665	4.210	-1.122	1.31	-5.606	0.105
F_2	-4.161	3.414	-9.820	1.224	-5.500	0.108
F_3	-0.717	0.892	-0.388	0.731	-4.962	0.161

Elastic bands' static field

To represent the characteristics of the orthosis with elastic bands attached, the joint torques τ_{stiff} were calculated from (7) in order to compose the static field. At each point (x,y) in the arm's workspace the joint angles were calculated by inverse kinematics (see Appendix). On the basis of joint angles we calculated elastic bands' lengths, corresponding forces and joint torques. Thereby, the value of stiffness-based orthosis was calculated by (8) and located at (x,y).

$$\tau_{static\ field}(x, y) = \sqrt{\tau_{stiff}^T \tau_{stiff}} \quad (8)$$

Starting and target points

Six starting/target points were chosen in the relatively narrow workspace in front of the subject as shown in Figure 1 and 2. On the basis of these points, six movement directions were selected: AB, AC, AD, FB, ED and EF. Movement distances between a set of starting and target points are shown in Table 3.

Procedure

The subject was asked to perform a task necessitating arm reaching movements in the horizontal plane. To ensure a comparable movement time durations, we used a metronome, which was set to 50 beats per minute (50 BPM, i.e. 1.2 seconds per beat). Every direction was repeated from 15 to 25 times meaning that the beats represent doing movements and resting alternately, for example: movement AB, rest at B, movement BA, rest at A, etc. We analyzed only the directions which are presented in Figure 1 and in Table 3.

Table 3 Movement directions and its distances.

Direction	Distance *[m]*
AB	0.39
AC	0.33
AD	0.28
FB	0.42
ED	0.47
EF	0.44

Note: The selected starting and target points are A=(-0.20, 0.24), B=(0.02, 0.56), C=(-0.19, 0.57), D=(-0.35, 0.48), E=(0.05, 0.34), F=(-0.39, 0.33) *[m]*.

Results

The results of our experiment are shown in Figure 4, where all hand trajectories and its velocity profiles are collected. Figure 4a shows hand trajectories in the case the elastic bands were not attached (intact trajectories) on the orthosis, but the subject also carried the orthosis. It could be seen that the intact trajectories are slightly curved. Different situation is shown in Figure 4b, where hand trajectories are significantly more curved (stiff trajectories). In this case, the elastic bands were attached on the orthosis. Hand tangential velocities are mostly bell-shaped, but there are some small differences between them. Hand tangential velocities for intact trajectories exhibit smooth single-peaked profiles, where peak is moved slightly to the left, while hand tangential velocities for stiff trajectories shows somewhat distorted bell-shaped pattern with one or two peaks. The latter velocity profiles do not have its peak moved strictly to one side. The trajectories are highly repeatable, which is a good indicator for the trajectories' optimality, especially in stiff trajectories, which we were investigating. Therefore, all groups of trajectories were averaged and shown as bold trajectories.

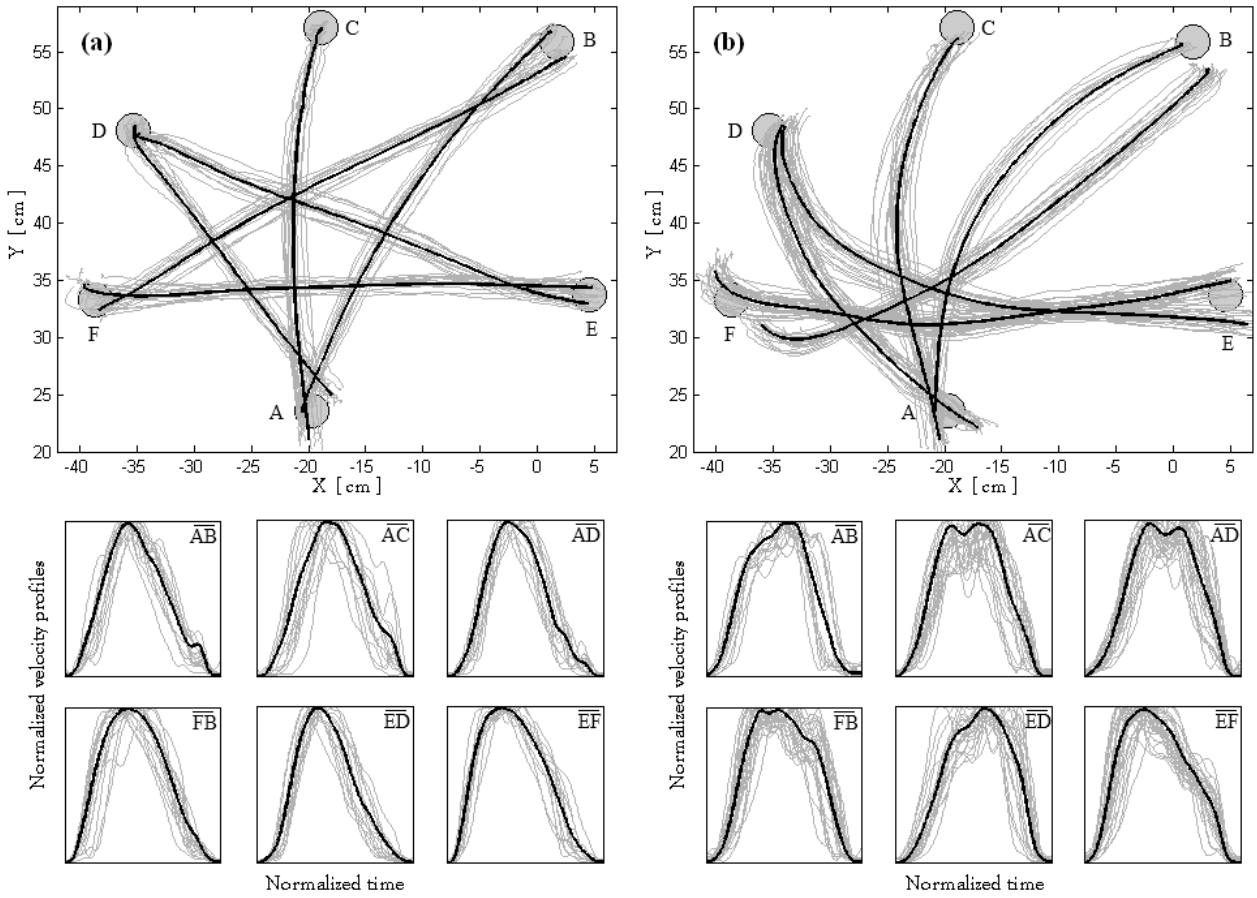

Figure 4 Experimentally obtained arm reaching trajectories and velocity profiles under (a) normal and (b) stiff arm conditions.

Below the X-Y graphs in Figure 4, there are corresponding normalized velocity profiles for each direction collected. Also, the average of velocity profiles were calculated and shown in bold. During movement recording the shoulder marker stayed most of the time within the circle with approximately 1 cm in diameter. It could be seen that starting and target positions of the recorded trajectories are not always reaching the marked positions (A~F), because it is hard to locate the exact marker position with the motion marker on the top of the hand.

By setting the metronome to 50 BPM, the trajectory durations of experimental movements were 1.11 s in average with standard deviation of 0.19 s.

Figure 5 shows the static field, which was calculated on the basis of human arm model with orthosis by (8). As an example, the experimental average trajectories of intact and stiff arm conditions of movement ED (direction 5) are shown on the top of the elastic bands' static field. The stiff trajectory is significantly more curved than the intact trajectory. The minimum zone of the static field is located on the near left side of the subject and its higher values are spreading with the elbow and shoulder extension to the right side of the subject. The values in the upper right zone are higher than 13 Nm.

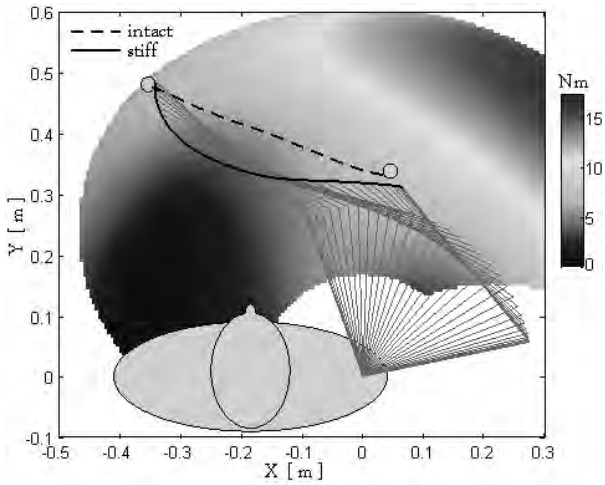

Figure 5 Comparison of intact (dashed line) and stiff (solid line) experimental trajectory with the elastic bands' static field in the background.

Discussion

This paper reports the results of experiment in which one subject was instructed to move the hand from selected starting to target point of the relatively narrow workspace in front. Two different arm conditions were considered. First, the trajectories of normal/intact arm were recorded (Figure 4a) and second, as an emulation of flexor contracture of the human arm, the subject carried orthosis, to which we attach elastic bands and then the i.e. stiff trajectories were recorded. Since we investigated the arm point-to-point reaching movements from the phenomenological point of view, the exact characteristics of elastic bands were not essential. As shown by the overlapping of the hand for the same movement directions, the subject produced relatively consistent movements, which was a sufficient reason to averaging the trajectories. The obtained trajectories between intact and stiff condition were significantly different. From the Figure 4b and Figure 5 it could be seen that the gradient of the trajectories' curvature were in the direction of minimum torques static field. As shown in Figure 4a, intact hand trajectories are not quite straight, but slightly curved with the bell-shaped velocity profiles. This is also evidenced by many other experimental[7,8] and minimum torque/torque-change simulation studies.[3,4] However, when we add the elastic bands, these trajectories become significantly different. This finding might be useful in rehabilitation after stroke.

Conclusion

The studies of human arm motion are essential for developing robot arms that interact with human subject. A clear understanding of human arm motion will aid for better interaction in between a machine and a human subject.[2] To promote effective rehabilitation after brain injury, a key element is intensive training, which is also facilitated by upper extremity rehabilitation robots such as many commercial devices.[9] In addition to the rehabilitation methods such as constraint induced movement therapy, functional electrical therapy, and assist-as-needed algorithms for rehab-robots, the planning trajectories, which take into account the patient's condition, are as much important. By knowing the characteristics of the impaired upper extremity (e.g. static field in Figure 5), we may also select the appropriate starting and target points, and then the calculation or optimization process to find the optimal trajectory between them. Eventually, the starting and target points and optimal trajectories could be properly planned over the several-weeks rehabilitation training.

Acknowledgements

We thank the Center for Prosthetics and Orthotics of the University Rehabilitation institute, Republic of Slovenia, for producing the the arm orthosis. The study was supported by the grant of the Slovenian Research Agency - ARRS research project P2-0228 and L2-2259.

References

1. Flash T, Hogan N: The Coordination of Arm Movements: An Experimentally Confirmed

Mathematical Model. *J Neurosci* 1985; 5: 1688-1703.
2. Amirabdollahian F, Loureiro R, Harwin R: Minimum Jerk Trajectory Control for Rehabilitation and Haptic Applications. *IEEE Conf. on Robotics and Automation – ICRA* 2002; 4: 3380-3384.
3. Uno Y, Kawato M, Suzuki R: Formation and control of optimal trajectories in human multijoint arm movements: Minimum torque-change model. *Biol Cybern* 1989; 61: 89-101.
4. Ohta K, Svinin MM, Luo Z, *et al.*: Optimal trajectory formation of constrained human arm reaching movements. *Biol Cybern* 2004; 91: 23-36.
5. Emken JL, Bobrow JE, Reinkensmeyer DJ: Robotic movement training as an optimization problem designing a controller that assists only as needed. *9th International Conf. on Rehabil. Robotics – ICORR* 2005; 307-312.
6. Zadravec M, Matjačić Z: The influence of haptic support algorithm dynamics on the efficacy of motor learning. *Zdrav Vestn* 2011; 80: 561-570.
7. Suzuki M, Yamazaki Y, Mizuno N, *et al.*: Trajectory formation of the center-of-mass of the arm during reaching movements. *Neuroscience* 1997; 76(2): 597-610.
8. Morasso P: Spatial Control of Arm Movements. *Exp Brain Res* 1981; 42: 223-227.
9. Hesse S, Schmidt H, Werner C, *et al.*: Upper and lower extremity robotic devices for rehabilitation and for studying motor control. *Curr Opin Neurol* 2003; 16: 705-710.

Appendix

The kinematics of elastic bands is expressed by orthosis parameters given in Table 1. Here, the lengths l_1, l_2 and l_3 are joint angular dependent parameters and defined as follows:

$$\left.\begin{aligned} l_1 &= \sqrt{A_1^2 + B_1^2 - 2A_1B_1\cos\varphi_1} \\ A_1 &= \sqrt{a_1^2 + b_1^2} \\ B_1 &= \sqrt{a_2^2 + b_2^2} \\ \varphi_1 &= \pi - \arctan\tfrac{b_1}{a_1} - \arctan\tfrac{b_2}{a_2} - \theta_1 \end{aligned}\right\}, \quad (9)$$

$$\left.\begin{aligned} l_2 &= \sqrt{A_2^2 + B_2^2 - 2A_2B_2\cos\varphi_2} \\ A_2 &= \sqrt{(L_1 - a_2)^2 + b_2^2} \\ B_2 &= \sqrt{a_3^2 + b_3^2} \\ \varphi_2 &= \pi - \arctan\tfrac{b_2}{L_1 - a_2} - \arctan\tfrac{b_3}{a_3} - \theta_2 \end{aligned}\right\}, \quad (10)$$

$$\left.\begin{aligned} l_3 &= \sqrt{A_1^2 + B_3^2 - 2A_1B_3\cos\varphi_3} \\ B_3 &= \sqrt{L_1^2 + B_2^2 - 2L_1B_2\cos\varphi_4} \\ \varphi_3 &= \pi - \arctan\tfrac{b_1}{a_1} - \arcsin\left(\tfrac{B_2}{B_3}\sin\varphi_4\right) \\ \varphi_4 &= \pi - \arctan\tfrac{b_3}{a_3} - \theta_2 \end{aligned}\right\}. \quad (11)$$

The inverse kinematics are defined as

$$\begin{bmatrix}\theta_1 \\ \theta_2\end{bmatrix} = \begin{bmatrix}\arctan 2(y,x) - \arccos\left(\frac{r^2 + L_1^2 - L_2^2}{2L_1 r}\right) \\ \pi - \arccos\left(\frac{L_1^2 + L_2^2 - r^2}{2L_1L_2}\right)\end{bmatrix}, \quad (12)$$

where

$$r = \sqrt{x^2 + y^2}\ ; \quad (13)$$

$$\arctan 2(y,x) = \arctan\left(\tfrac{y}{x}\right) + \operatorname{sgn}(y)\left(1 - \operatorname{sgn}(x)\right)\tfrac{\pi}{2}. \quad (14)$$